MAGNETICALLY ACTUATED MICROMIRRORS for FIBER-OPTIC SWITCHING

Behrang Behin, Kam Y. Lau, and Richard S. Muller
Berkeley Sensor & Actuator Center (BSAC)
Department of EECS, University of California
Berkeley, CA 94720-1770

ABSTRACT

We describe the design, fabrication, and operation of magnetically actuated micromirrors with electrostatic clamping in dual positions for fiber-optic switching applications. The mirrors are actuated by an off-chip electromagnet and can be individually addressed by electrostatic clamping either to the substrate surface or to the vertically etched sidewalls formed on a top-mounted (110)-silicon chip. We show that the positioning accuracy inherent in our approach makes it suitable for NxM optical switches.

INTRODUCTION

The growth of fiber-optic communications networks and the increased use of fiber-optics in sensing applications has created demand for low-loss, low-cost, reliable, and mass-producible fiber-optic switches. Free-space optical switches are needed for multi-mode fiber switching and for applications that require lower crosstalk than that provided by waveguide-based electro-optical switches. A significant opportunity exists for MEMS in the realization of low-cost free-space optical switches [1,2]. Batch-processing and –assembly make MEMS especially suitable for large-scale switching applications such as NxM fiber-optic non-blocking switches. A number of authors have described NxM switches based on silicon surface- and bulk-micromachining [3-6].

A MEMS design for an NxM switch is a matrix of micromirrors arranged in a crossbar configuration, as shown in Fig. 1 [3]. The mirrors are positioned at 45° relative to the fiber/collimator arrays. Once flipped vertically, a mirror reflects the collimated output from an input fiber into an output fiber. Accuracy of the mirror angle in the vertical position is a major challenge to the efficacy of this design. Assuming that the fiber/collimator arrays are perfectly orthogonal, all mirrors must have the same vertical angle to achieve a low insertion loss. Reproducibly accurate positioning of the mirrors requires either the use of active positioning control or of mechanical stops. The latter design can be accomplished with less complexity, but may require several precise alignment steps during system assembly. We describe a design that only demands a single alignment step of the MEMS mirror assembly to the fiber/collimator arrays.

OPTICAL DESIGN CONSIDERATIONS

A major parameter describing an optical switch is its insertion loss. For the NxM crossbar switch shown in Fig. 1, separation between the fiber/collimator assemblies and misalignment of the mirrors both result in coupling losses. Fiber collimators (lenses) are used to expand the beam radius to *fN.A.*, where *f* is the lens focal length and *N.A.* is the numerical aperture of the fiber. Use of these collimators reduces sensitivity to lateral misalignment of the fibers, so we can model coupling sensitivity as resulting only from separation and angular mismatch.

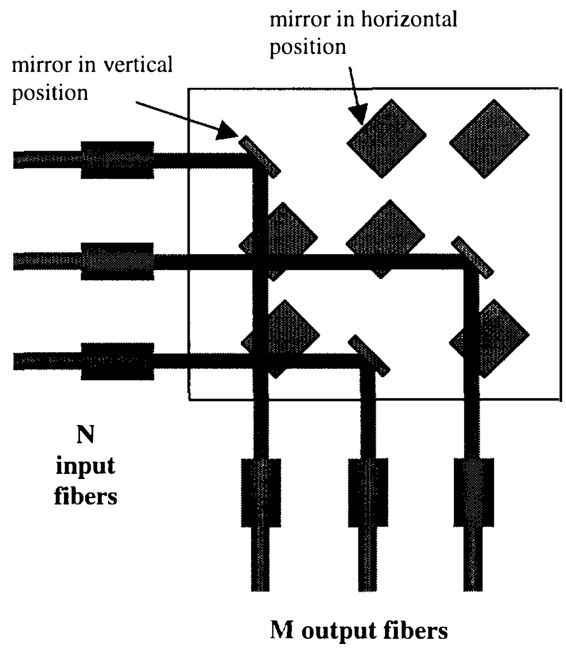

Figure 1. *MEMS design concept for a 3x3 crossbar optical switching network.*

For a fiber placed at the focal plane of a lens, as shown in Fig. 2(a), the output beam has angular divergence *a/f*, where *a* is the fiber core radius. As the beam traverses a distance *s* to another fiber/collimator assembly, the spot radius increases from (*fN.A.*) to (*fN.A.* + *as/f*), resulting in coupling loss between the two fibers. Loss due to angular misalignment is illustrated in Fig. 2(b). The image of a beam incident on the collimator at an angle θ is projected onto the fiber end-face with a lateral translation relative to the fiber core. Note that for reflection from a mirror, θ is twice the angular misalignment of that mirror. Coupling loss due to angular mismatch is higher for fibers having smaller core radii because the lateral translation of the projected image is larger relative to the core radius.

Detailed treatments of coupling loss between fibers due to separation, lateral misalignments, and angular mismatches have been used to model coupling in free-space optical interconnects [7,8]. The data in Fig. 3 were generated for typical parameters expected in a MEMS 3x3 switch array using analytical approximations developed by di Vita *et. al.* and Rossi in references 7 and 8. Although our analysis is based upon expressions derived for multi-mode fibers, we also generate data for single-mode fibers to establish rough guidelines and evaluate tradeoffs for the design of a MEMS crossbar switch. The plots in Fig. 3 show coupling efficiency η *vs.* θ for two fibers with different core radii, each with two lenses of differing focal lengths. For the single-mode case, a

0-9640024-2-6/hh1998/$20©1998TRF
DOI 10.31438/trf.hh1998.62

Solid-State Sensors, Actuators, and Microsystems Workshop
Hilton Head Island, South Carolina, June 8-11, 1998

smaller core radius results in less beam spreading and higher maximum efficiency. However, a smaller core radius also makes η more sensitive to angular misalignments. For both fibers, a shorter focal length results in lower sensitivity to angular mismatch; however, the coupling loss at θ = 0 is higher for shorter focal lengths because of beam spreading. To use a longer focal length

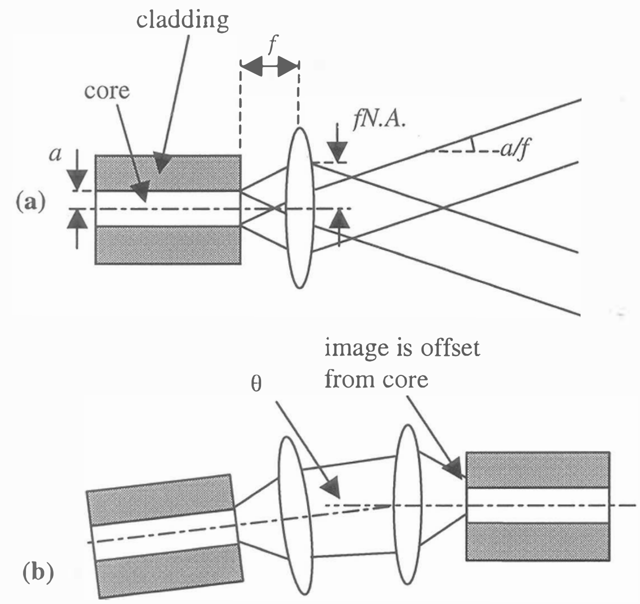

Figure 2. **(a)** *Beam divergence for fiber/collimator assembly.* **(b)** *Beam image projection is offset from core owing to angular mismatch.*

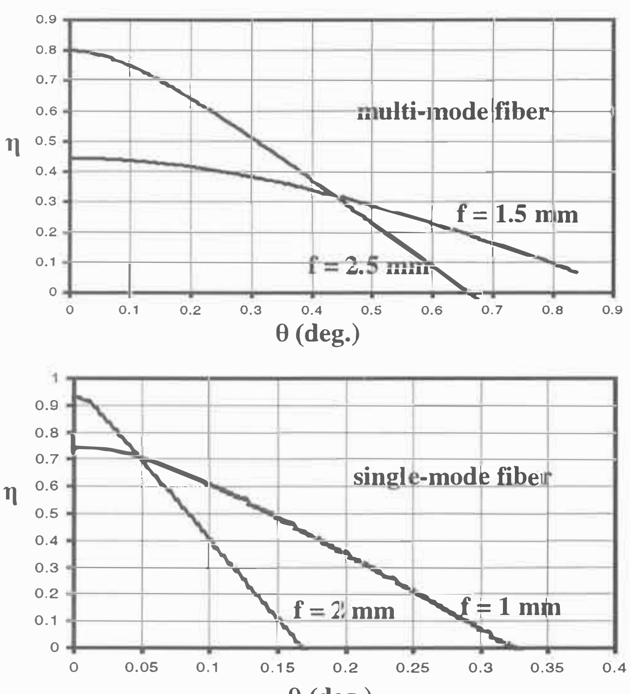

Figure 3. *Simulated approximate coupling efficiency vs. angular mismatch for different fiber/collimator assemblies. θ is twice the angular misalignment of the mirror. In all cases, N.A. = 0.1, and s = 1 cm. The fiber core radius is 25 μm in the top graph and 5 μm in the bottom graph.*

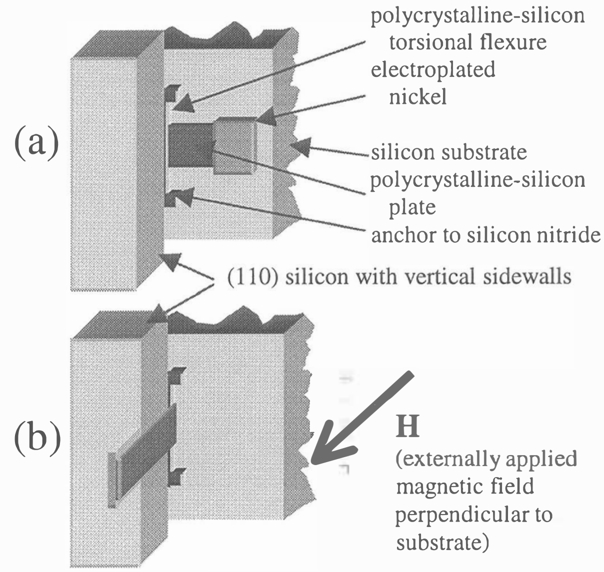

Figure 4. *Torsion-bar-mounted magnetic mirror with (110)-oriented silicon chip bonded on the base chip, shown in its horizontal and vertical position.*

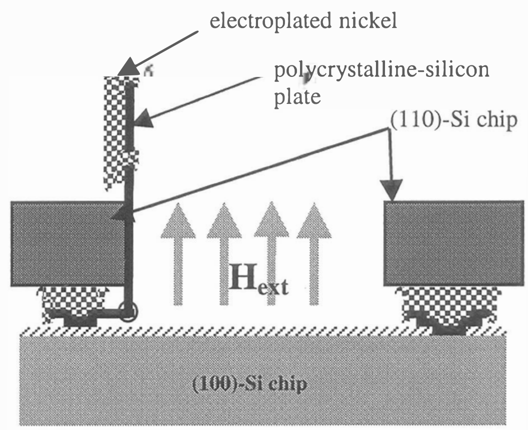

Figure 5. *Cross section of mirror assembly.*

(for improved coupling efficiency), a tighter angular tolerance must be maintained. From the analysis summarized in Fig. 3, we conclude that coupling is extremely sensitive to the beam angular incidence. For example, for an insertion loss of 3 dB, the mirrors in a typical MEMS 3x3 switch must be positioned with ~0.15° accuracy for multi-mode fibers and ~0.08° accuracy for single-mode fibers.

DESIGN

To control the vertical mirror angle precisely, we employ electrostatic clamping of magnetically actuated torsion-bar-mounted mirrors to vertical sidewalls of an anisotropically etched (110)-silicon top-mounted structure. Previous work has established that magnetically actuated mirrors can be clamped electrostatically to the substrate [11,12]. In references 11 and 12, mirrors were either torqued out of the substrate plane by an external electromagnet or selectively kept in the horizontal position by applying a voltage between the mirrors and the substrate. In this work, we introduce a vertical clamping structure, as shown in Fig. 4, to fix the "mirror-up" position. We insure uniformity of the vertical-mirror angle over the entire device by employing selective

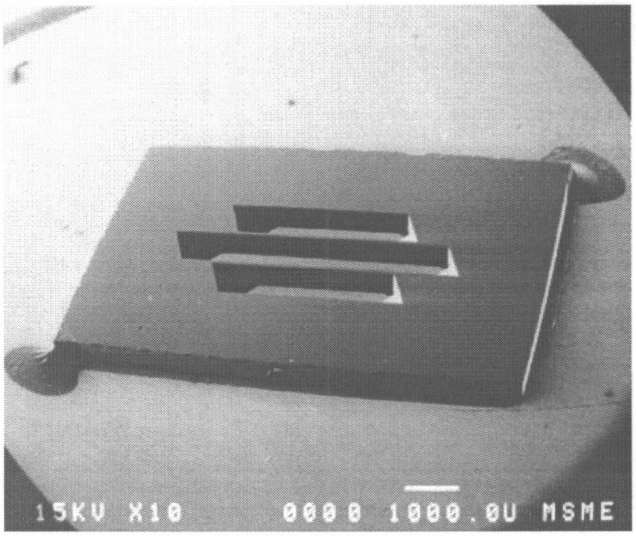

Figure 6. *SEM image of KOH-etched (110)-silicon chip for electrostatic clamping of magnetic torsion mirrors.*

etching along the <110> crystal axis [9,10] to define the precise orientation of the vertical clamping electrodes.

Vertical clamping also allows us to address individual mirrors in an NxM mirror matrix independently. Figure 4 shows the mirror in its two positions. A field (typically ~300 Gauss) applied from an external magnet actuates the mirror between these two positions by applying a force on the magnetized nickel plate situated on the top portion of the mirror structure. An applied voltage (typically 15 to 25 V) can be used to clamp the mirror by electrostatic forces that exceed those from the magnetic field. Hence, every mirror can be individually switched between its two positions without disturbing any of the other mirrors.

FABRICATION

The mirror assembly is built up of two silicon chips: a (100)-silicon chip on which the surface-micromachined mirrors are fabricated, and a (110)-silicon chip containing via-holes with vertically etched sidewalls. The surface-micromachined mirrors consist of polycrystalline-silicon plates that are anchored to the substrate by two torsion flexures. The top parts of the plates are electroplated with nickel to interact with the magnetic field. Low-stress silicon nitride electrically isolates the mirrors from the substrate. A more detailed description of mirror fabrication and actuation is provided by Judy *et. al.* [11,12].

The top-mounted (110)-silicon structure is formed by KOH anisotropic etching. First, a radial pattern of rectangular openings at 0.05° increments along the wafer perimeter is defined in a 0.12 μm-thick silicon nitride etch mask. The exposed silicon is etched 200 μm deep using KOH to produce a series of pits along the wafer perimeter. Those openings having edges parallel to the (111) planes give rise to pits having the minimum mask undercut [13]. A second mask is aligned to the pits with minimal mask undercut (and hence to the (111) planes) and used to define larger openings in the silicon nitride. A subsequent KOH etch forms via holes having vertical sidewalls. The etch is carried out using a mixture of 30% KOH and water at 80 °C, resulting in an etch rate of ~2.4 μm/min for the (110) planes and 100:1 selectivity to the perpendicular (111) planes. The bath is stirred and the wafers are rotated 90° every 30 minutes to insure uniform etching across the wafer. The degree of undercut below the silicon nitride etch mask (due to etching of the (111) planes) is used to infer the uniformity of the vertical-sidewall-angle (average deviation ≈ 0.015° across wafer). Finally, the silicon nitride mask is removed and 160 nm of thermal oxide is grown on the wafer. Figure 6 is an SEM of a chip designed for a 2x2 switch. A stylus scan along the length of the sidewall reveals 300 nm irregularities that repeat every 0.5 mm. These steps are due to slight misalignment of the second mask to the crystal [13].

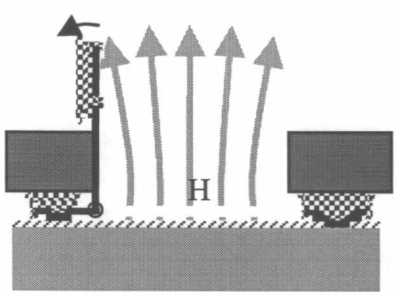

Figure 7. *A magnetic field that is not perfectly vertical can induce bending in vertically clamped mirrors.*

To address the individual mirrors independently, mirrors in the vertical position must be unaffected by the switching of other mirrors. A problem arises when the field is not perfectly parallel

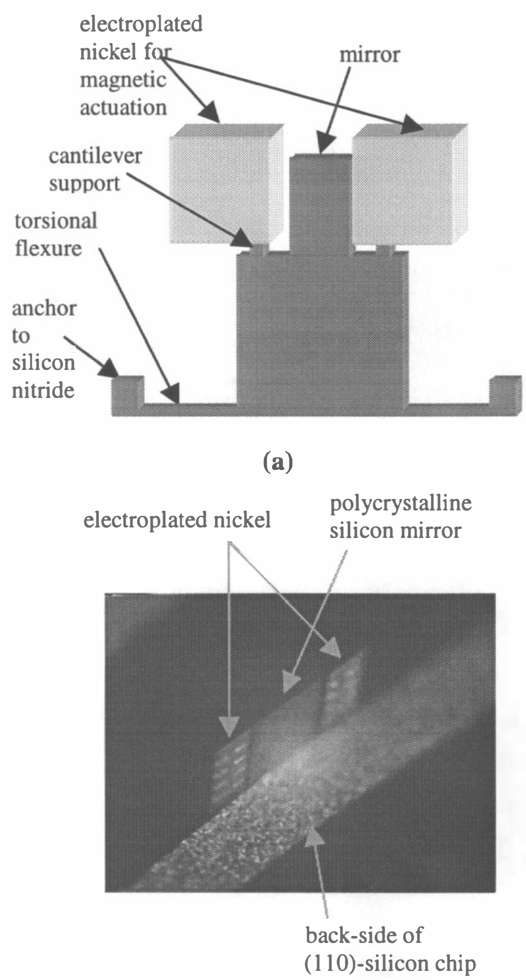

Figure 8. **(a)** *Design to reduce effect of magnetic torque on vertically clamped mirrors. The electrodeposited nickel thickness has been exaggerated.* **(b)** *Mirror clamped vertically to (110)-silicon structure.*

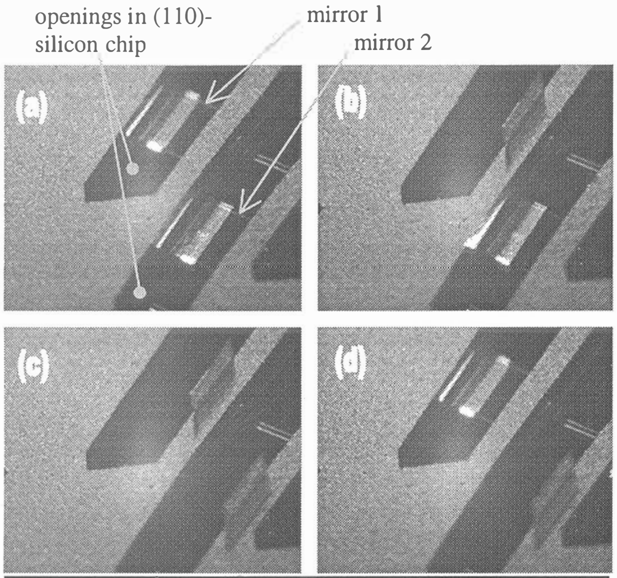

Figure 9	Mirror 1 Voltage	Mirror 2 Voltage	Magnetic Field
(a)	on	on	off
not shown	off	on	on
(b)	on	on	off
not shown	on	off	on
(c)	on	on	off
(d)	off	on	off

Figure 9 and Table 1. *Mirror operation and individual addressing.*

to the vertical mirror position. In Fig. 7, the divergence of the external field is exaggerated to illustrate this effect. A non-parallel magnetic field induces a slight torque and resultant bending in vertically clamped mirrors, causing misalignment of the reflected beams.

The design shown in Fig. 8(a) reduces bending effects on optical performance by mechanically isolating the reflecting surface from the nickel plates. The magnetically active portion of the mirror is connected to the rest of the structure by narrow support arms that isolate the mirror surface from the forces on the nickel plates when the mirror is clamped vertically. Mirrors of the design shown in Fig. 8(a) are shown clamped vertically in Fig. 8(b). These mirrors show significantly smaller bending effects in response to non-vertical magnetic fields. For these prototype mirrors, reflection was taken directly from the silicon surface.

MIRROR OPERATION

Mirror switching, as shown in Fig. 9, is implemented by an off-chip electromagnet. Both substrates are kept at electrical ground and clamping voltages are applied to individual mirrors to hold them either in vertical or horizontal positions. We have found that ac voltages (typically square waves above 250 Hz) result in more reliable operation than does pure dc clamping. The nature of this effect is under study.

The mirrors are approximately 1 mm^2, with 1100 x 400 x 10 μm nickel plates and 15 x 500 x 1.9 μm torsion flexures. They are actuated by a ~320 Gauss magnetic field and clamped with a 15 V amplitude 1 kHz square-wave. The vertical mirror angle (with the electromagnet off) for a single mirror was measured by monitoring the reflected beam with a position-sensitive photodetector and was found to be reproducible to within ~0.04°. Switching rates are presently under study.

In Fig. 9(a), both mirrors are clamped horizontally. The clamping voltage for mirror 1 is turned off and the electromagnet is turned on to swing it vertically. Next, the clamping voltage for mirror 1 is turned on and the electromagnet turned off (Fig. 9(b)). With mirror 1 clamped vertically, mirror 2 is flipped vertically and clamped (Fig. 9(c)). In Fig. 9(d), the voltage on mirror 1 is turned off and the torsion flexures force the mirror to the horizontal position.

CONCLUSIONS

We have demonstrated magnetically actuated micromirrors with electrostatic clamping in dual positions. Rough calculations show that fiber-optic switching applications require precise control of the mirror angle ($\lesssim$0.15° for multi-mode fibers and $\lesssim$0.08° for single-mode fibers to achieve 3 dB insertion loss). We have shown that employing vertically etched sidewalls of a top-mounted (110)-silicon chip to electrostatically clamp the mirrors can achieve the positioning accuracy necessary for fiber-optic switching applications. The top-mounted bulk-machined chip also allows single-step parallel assembly of all mirrors in an NxM matrix.

ACKNOWLEDGMENTS

The fabrication was carried out at the U.C. Berkeley Microlab, and we thank Microlab staff, especially Jim Bustillo, for technical assistance. Carl Chang provided help with nickel electroplating, and Kris Pister and Chris Keller gave helpful technical discussions.

REFERENCES

1. K. Y. Lau, "MEM's the word for optical beam manipulation," *IEEE Circuits and Devices*, vol. 13, no. 4, 11-8, July 1997.
2. M. C. Wu, "Micromachining for optical and optoelectronic systems," *Proc. IEEE*, vol. 85, no. 11, 1833-56, Nov. 1997.
3. H. Toshiyoshi and H. Fujita, "Electrostatic micro torsion mirrors for an optical switch matrix," *J. Microelectromech. Syst.*, vol. 5, no. 4, 231-7, Dec. 1996.
4. S.-S. Lee and M. C. Wu, "Surface-micromachined vertical torsion mirror switches," *Tech. Dig. MOEMS97*, 115-8, 1997.
5. C. Marxer, C. Thio, N. F. de Rooij, O. Anthamatten, R. Battig, B. Valk, P. Vogel, "Micro-opto-mechanical 2x2 switch for single mode fibers based on plasma-etched silicon mirror and electrostatic actuation," *Tech. Dig. MOEMS97*, 233-7, 1997.
6. W. H. Juan and S. W. Pang, "Batch-micromachined, high aspect ratio Si mirror arrays for optical switching applications," *Transducers '97*, 93-6, 1997.
7. P. di Vita and U. Rossi, "Theory of power coupling between multimode optical fibers," *Opt. Quantum Electron.*, vol. 10, 107, 1978.
8. A. Nicia, "Lens coupling in fiber-optic devices: efficiency limits," *Applied Optics*, vol. 20, no. 18, 3136-45 Sep. 1981.
9. Y. Uenishi, M. Tsugai and M. Mehregany, "Micro-opto-mechanical devices fabricated by anisotropic etching of (110) silicon," *J. Micromech. Microeng.* 5, 305-12, 1995.
10. R. A. Miller, Y.-C. Tai, G. Xu, J. Bartha, and F. Lin, "An electromagnetic MEMS 2x2 fiber optic bypass switch," *Transducers'97*, 89-92, 1997.
11. J. W. Judy and R. S. Muller, "Batch-fabricated, addressable, magnetically actuated microstructures," *Tech. Dig. Solid-State Sensor and Actuator Workshop*, 187-90, 1996.
12. J. W. Judy and R. S. Muller, "Magnetically Actuated, Addressable Microstructures" *J. Microelectromech. Syst.*, vol. 6, no.3, pp. 249-56, 1997.
13. D. L. Kendall, "On etching very narrow grooves in silicon," *Appl. Phys. Lett.*, vol. 26, no. 4, 195-8, Feb. 1975.